Trans Indian Inst Met (2016) 69(10):1811–1818
DOI 10.1007/s12666-016-0841-8

TECHNICAL PAPER

Microstructure and Mechanical Characterization of Aluminum Seamless Tubes Produced by Friction Stir Back Extrusion

N. Mathew[1] · I. Dinaharan[2] · S. J. Vijay[1] · N. Murugan[3]

Received: 28 July 2015 / Accepted: 31 January 2016 / Published online: 18 February 2016
© The Indian Institute of Metals - IIM 2016

Abstract Friction stir back extrusion (FSBE) is emerging as a novel method to produce high strength fine grained metallic tubes. The objective of the present work is to produce aluminum seamless tubes from solid cylindrical bars using FSBE and to report the microstructure and mechanical characterization. A die, tool and fixture were designed to carry out FSBE. A conventional friction stir welding machine was utilized for FSBE. A cylindrical bar of aluminum alloy AA6061-T6 was kept inside the hole in the die and extruded by plunging the rotating tool. The microstructure of the produced tube was studied using optical microscopy. The microstructure was found to be homogeneous along the tube. The microhardness and compressive strength of the tube have been presented in this paper. The results indicated that the FSBE process was capable of producing sound aluminum seamless tubes.

✉ I. Dinaharan
dinaweld2009@gmail.com

N. Mathew
mnoblem@gmail.com

S. J. Vijay
vijayjoseph.2001@gmail.com

N. Murugan
drnmurugan@gmail.com

[1] School of Mechanical Sciences, Karunya University, Coimbatore, Tamil Nadu 641114, India

[2] Department of Mechanical Engineering Science, University of Johannesburg, Auckland Park Kingsway Campus, Johannesburg 2006, South Africa

[3] Department of Mechanical Engineering, Coimbatore Institute of Technology, Coimbatore, Tamil Nadu 641014, India

Keywords Aluminum alloys · Friction stir back extrusion · EBSD · Microstructure

1 Introduction

Friction stir welding (FSW) is a novel solid state welding technique invented at The Welding Institute (TWI), UK in 1991 [1]. Frictional heat is utilized to deform the material plastically and forge under sufficient axial force to create a joint. The plates to be joined are clamped rigidly in a fixture and a non consumable rotating tool harder than the base material is plunged at one end of the joint line. The tool is then traversed along the joint line after a short dwell period. The rubbing of the tool shoulder on the base material and shearing of material by the tool pin generates frictional heat. The plasticized material is transported from one side of the tool to the other side to complete the joint [2, 3]. FSW was invented to join aluminum alloys, but rigorous research work enabled FSW to join various other monolithic materials including magnesium [4], copper [5], nickel [6], steel [7] titanium [8] and zirconium [9]. The highlight of FSW process is the generation of ultra fine grained (UFG) structure in the weld zone induced by severe plastic deformation (SPD). Cavaliere et al. [10] reported the average grain size of friction stir welded aluminum alloy AA6056 to be 4–5 μm. Hatamleh et al. [11] observed a grain size of 5–12 μm in friction stir welded aluminum alloy AA7075. Mishra et al. [12] utilized the SPD induced by FSW to generate fine grains in metallic materials and named the process as friction stir processing (FSP).

UFG materials possess enhanced physical and mechanical properties compared to their coarse grained counterparts [13]. A range of SPD processes have been investigated by researchers to produce UFG materials, including constrained groove pressing [14], accumulative

roll bonding [15], cyclic extrusion compression [16], high pressure torsion [17], equal channel angular pressing [18] and continuous repetitive corrugation and straightening [19]. It is not feasible to produce UFG tubular material using those processes. However, UFG tubular material can be produced from the limited available SPD processes such as accumulative spin bonding [20], tube channel pressing [21], high pressure tube twisting [22] and tubular channel angular pressing [23]. Nevertheless, FSP has attracted the attention of current researchers to produce UFG structure in metallic materials among the SPD processes. UFG materials are produced by FSP due to the intense stirring action of the tool at elevated temperature caused by frictional heat as well as deformation induced heat [24]. Since SPD occurs at elevated temperature in FSP, the load requirement and machine rigidity are relatively lower with respect to other SPD processes. Despite its merits, FSP cannot be applied to produce UFG tubular material.

A novel process based on the principles of FSP has emerged recently to produce metallic tubes with a fined grained structure. The process was developed by Farha [25] and was coined the term friction stir back extrusion (FSBE) in his first report. FSBE produces fine grained tubes from solid cylindrical bars in a single step. He was successful to produce sound aluminum alloy AA6063-T52 tubes by FSBE and observed a fine grain structure along the tube wall. Milner and Farha [26] demonstrated the feasibility to produce magnesium alloy AZ31 tubes using FSBE. Dinaharan et al. [27] applied FSBE to produce pure copper tubes of uniform wall thickness. The microstructure was found to be homogeneous along the copper tube. Khorrami and Movahedi [28] fabricated aluminum tubes using FSBE and identified several regions in the formed tube.

Tubular materials are vastly used in aerospace, automotive and petroleum industries worldwide [29]. At this point of time, FSBE process appears to be capable of producing high strength metallic tubes. However, the knowledge of this promising process is limited. Further works are needed to establish the process thoroughly across the spectrum of materials to expand the applications and commercialize the process. Therefore, the current work is focused to produce aluminum alloy AA6061-T6 tubes of internal diameter 19 mm and wall thickness 3 mm using FSBE by appropriate tool and die design and study the microstructure and mechanical properties.

2 Experimental Procedure

2.1 FSBE Principle

The FSBE principle is schematically shown in Fig. 1. A cylindrical bar was placed at the end of the circular hole in the die. A rotating tool was lowered to touch the top surface of the cylindrical bar. A dwell period was given for initial plasticization of the material to ease the extrusion process. After the short dwell period, the tool was plunged into the cylindrical bar at an axial feed. The stirring action combined with axial force imposed SPD on the material. The plasticized material escaped into the space between tool and die wall and formed the tube. The tool was finally retracted after extruding the tube to the brim of the hole in the die.

2.2 Design of Tool and Die

The FSBE setup as presented in Fig. 1 consisted of two main components, namely stirring tool and die. The fabricated tool and the die are shown in Fig. 2. A stirring tool of diameter 19 mm was designed and made of high carbon high chromium steel (HCHCr). The end of the tool was tapered to an angle of 10° to facilitate the extrusion process. The tapered angle could be treated equivalent to the extrusion angle in a conventional extrusion process. The die was designed in a cylindrical shape, split into two halves. The die was also made of the same material as that of tool and was tempered. A hole of 25 mm to a depth of 100 mm was drilled in the centre of the die. The total height of the die was 130 mm. A special fixture was made of mild steel to hold the die in position during FSBE.

2.3 Production of Aluminum Seamless Tubes

An indigenously built FSW machine (M/s RV Machine Tools, Coimbatore, India) was used for FSBE. The experimental

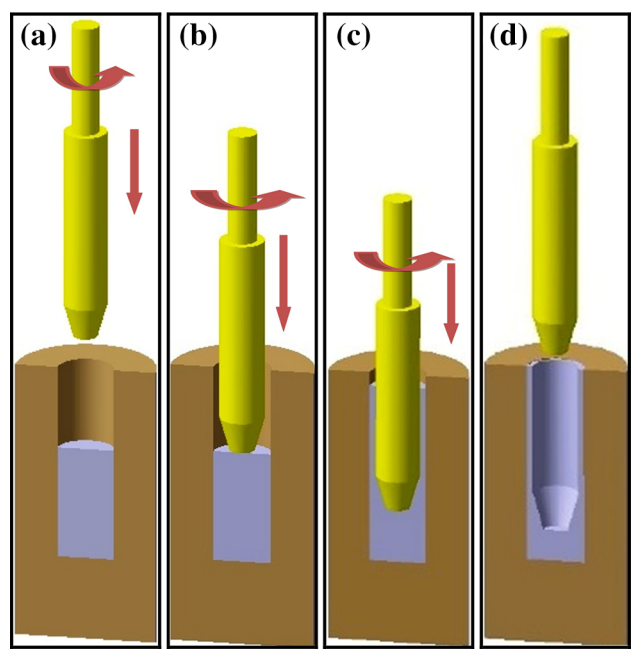

Fig. 1 Schematic of FSBE process; **a** lowering of rotating tool, **b** dwell period, **c** plunging of tool and **d** retraction of tool

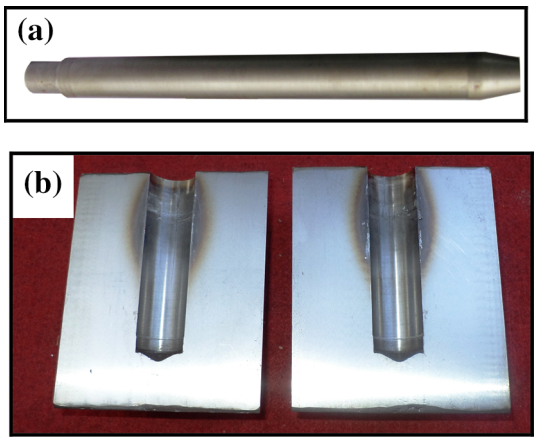

Fig. 2 Photograph of fabricated; **a** tool and **b** die for FSBE process

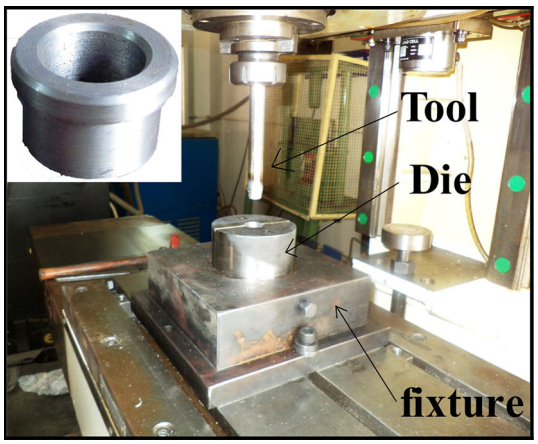

Fig. 3 Photograph of experimental set up. *Inset* shows the locator bush

setup is shown in Fig. 3. The fixture was secured to the machine bed. The die was placed on the fixture. A cylindrical extruded aluminum alloy AA6061-T6 bar of diameter 25 mm and height 50 mm was inserted into the hole in the die. The inside wall of the hole was lubricated initially to facilitate tube extraction. The composition of the aluminum alloy is presented in Table 1. The axis of the tool was aligned with the hole with the aid of a locator bush. The aluminum seamless tubes were extruded as per the procedure in Fig. 1. The tool was rotated at 1800 rpm with an axial feed of 1.5 mm/s. An axial force of 10 kN was applied on the tool. The dwell time was approximately 8 s. The extrusion ratio was 4.2. Neither the die, nor the cylindrical bar was preheated. The parameters were chosen based on trial experiments. Two tubes were prepared using the same set of parameters.

2.4 Characterization of Aluminum Seamless Tubes

One of the tubes was sliced into two halves using wire cut EDM. The cross section was polished as per standard metallographic procedure. The metallographically polished samples were electro polished in a mixture of perchloric acid and methanol for EBSD studies. EBSD was carried out in a FEI Quanta FEG SEM equipped with TSL-OIM software. The microhardness was measured using a microhardness tester (MITUTOYO-MVK-H1) at 500 g load applied for 15 s. Another tube of length 52.5 mm was used to estimate the ultimate compressive strength (UCS). The UCS was evaluated using a computerized universal testing machine.

3 Results and Discussion

3.1 Macrostructure of Aluminum Seamless Tubes

Aluminum alloy AA6061 tubes have been successfully produced by FSBE process. Typical views of aluminum seamless tube are depicted in Fig. 4. The top view (Fig. 4a) shows that the wall of the tube is formed completely. There are no cracks in the cross section. The outer view (Fig. 4b) of the aluminum seamless tube shows no visible defects. The surface is smooth and there are no discontinuities. Spiral markings are also observed, which gives evidence to the material flow during FSBE. The combined rotational and axial movement of the stirring tool forces the plasticized material to observe three dimensional spiral paths. The material experiences twisting during the formation of the tube. Farha [25] called this phenomena as spiral friction stir processing. His observation shows a lip like structure at the end of the tube. No such lip like structure is seen in Fig. 4b. Such a structure has been observed in trial tubes (Fig. 4b) in the absence of dwell period or allowed to extrude outside the die hole. Plunging of stirring tool without any dwell period results in jerking. The blackish appearance on tube surface (Fig. 4d) is due to the application of high temperature lubricant inside the die hole. The lubricant avoids sticking of the extruded aluminum seamless tube with the die. The cross section of the aluminum seamless tube along the extrusion direction is depicted in Fig. 4c. No internal defects are present. The figure shows a prismatic uniform tube. The wall thickness is uniform throughout the extrusion depth. The stirring tool has not been plunged throughout the depth of the hole in the die. A portion of the as received material has been left intentionally for metallurgical characterization. It is evident from Fig. 4 that FSBE process is capable of producing sound aluminum alloy AA6061 tubes.

3.2 Microstructure of Aluminum Seamless Tubes

The EBSD maps and the corresponding grain boundary maps of the aluminum seamless tube at several locations

Table 1 The chemical composition of AA6061-T6 alloy

Element	Mg	Si	Fe	Mn	Cu	Cr	Zn	Ni	Ti	Aluminium
wt%	0.95	0.54	0.22	0.13	0.17	0.09	0.08	0.02	0.01	Balance

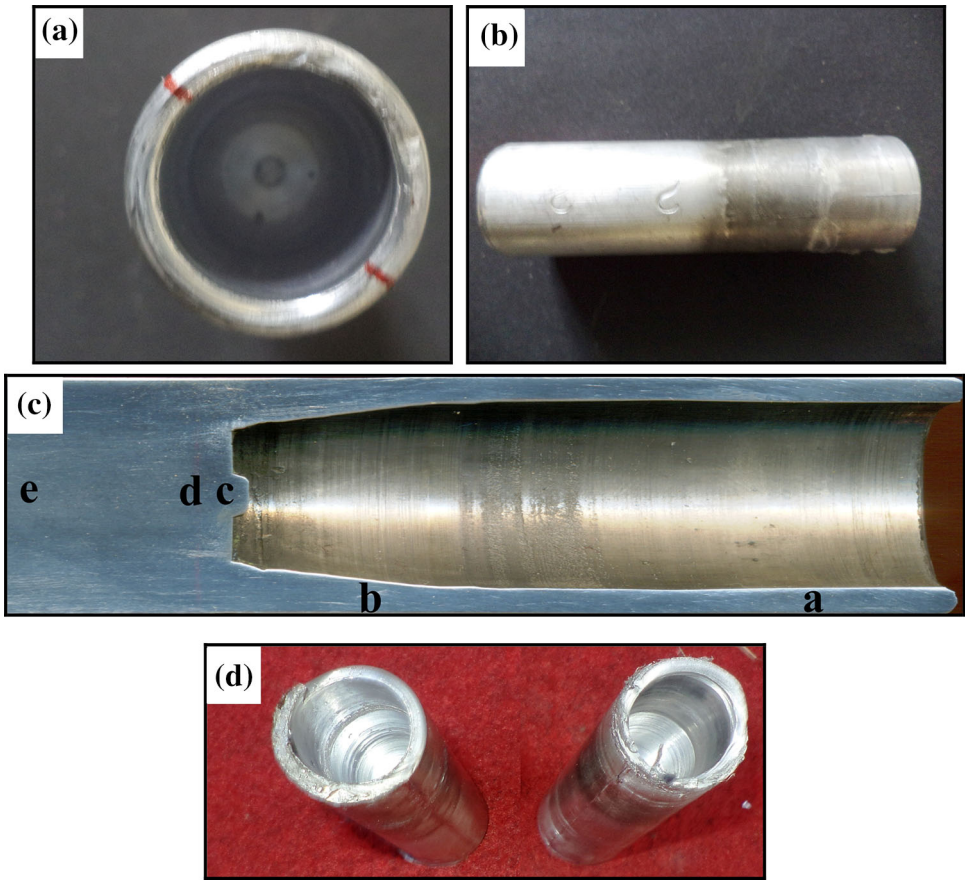

Fig. 4 Photograph of friction stir back extruded aluminum tubes; **a** inner view, **b** outside view, **c** cross sectional view along extrusion direction (notations are locations where EBSD was taken) and **d** trial tubes

are presented in Figs. 5 and 6. The microstructures of the tube wall at various locations are shown in Fig. 5a, b. The grains are highly elongated subsequent to the extrusion process. The average grain size is ~39 μm. The variation of the microstructure of the tube at different locations is negligible. FSBE process produces homogeneous aluminum seamless tubes. A stir zone is observed at the location marked as "c" in Fig. 4c. The stir zone microstructure is presented in Figs. 5c and 6c. Fine equiaxed grain structure is observed in this zone. The microstructure is analogous to the microstructure commonly observed in the weld zone of friction stir welded aluminum alloy AA6061 [30]. The stirring action of the tool creates intense plastic deformation and frictional heating. The result is a dynamically recrystallization phenomenon which is responsible for producing fine grain structure. The average grain size is ~3.5 μm. The depth of the zone is <1 mm under the center of the stirring tool. Khorrami and Movahedi [28] reported the depth of the stir zone to be 1.2 mm. The FSBE process parameters such as tool rotational speed, axial feed, extrusion ratio and tool geometry can have an influence on the depth of stir zone and material flow characteristics.

The stir zone is initially formed as the rotating tool rubs the cylindrical bar and is later extruded into tube wall. It is evident from Figs. 5 and 6 that the grain size of the tube wall is higher than the grain size of stir zone. In other words, considerable degree of coarsening of grains in the stir zone takes place subsequent to extrusion. The coarsening can be attributed to the characteristic of FSBE and its heat transfer. In the case of friction stir welding of aluminum alloy sheets, the stirring tool advances continuously. The welded zone undergoes cooling once the tool advances. But, the isolation of the extruded material from

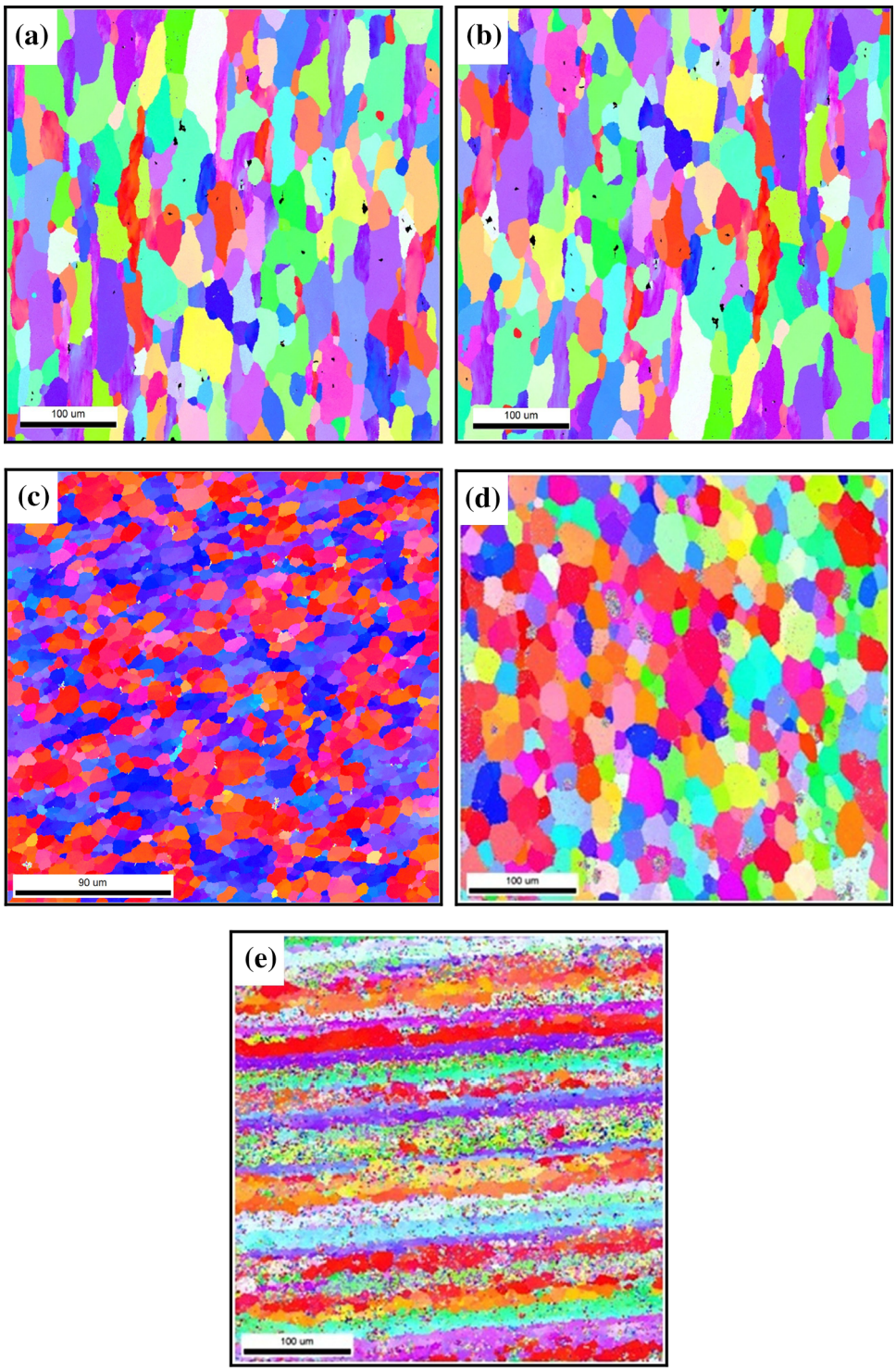

Fig. 5 EBSD map of: **a**, **b** tube wall, **c** stir zone, **d** intermediate zone and **e** as received AA6061

the die hole is not possible till the total extrusion is completed. The tube continues to be in contact with the stirring tool. There is no way for the generated frictional heat to dissipate, except to be trapped inside the die hole. The trapped frictional heat leads to grain growth. The result agrees with the findings of Farha [25]. This necessitates a cooling arrangement for the extruded tube during FSBE to control the microstructure evolution. A revised die design with internal cooling passages may be a remedy to alleviate grain coarsening.

An intermediate zone indicated by "d" in Fig. 5 is observed between the stir zone and the parent aluminum

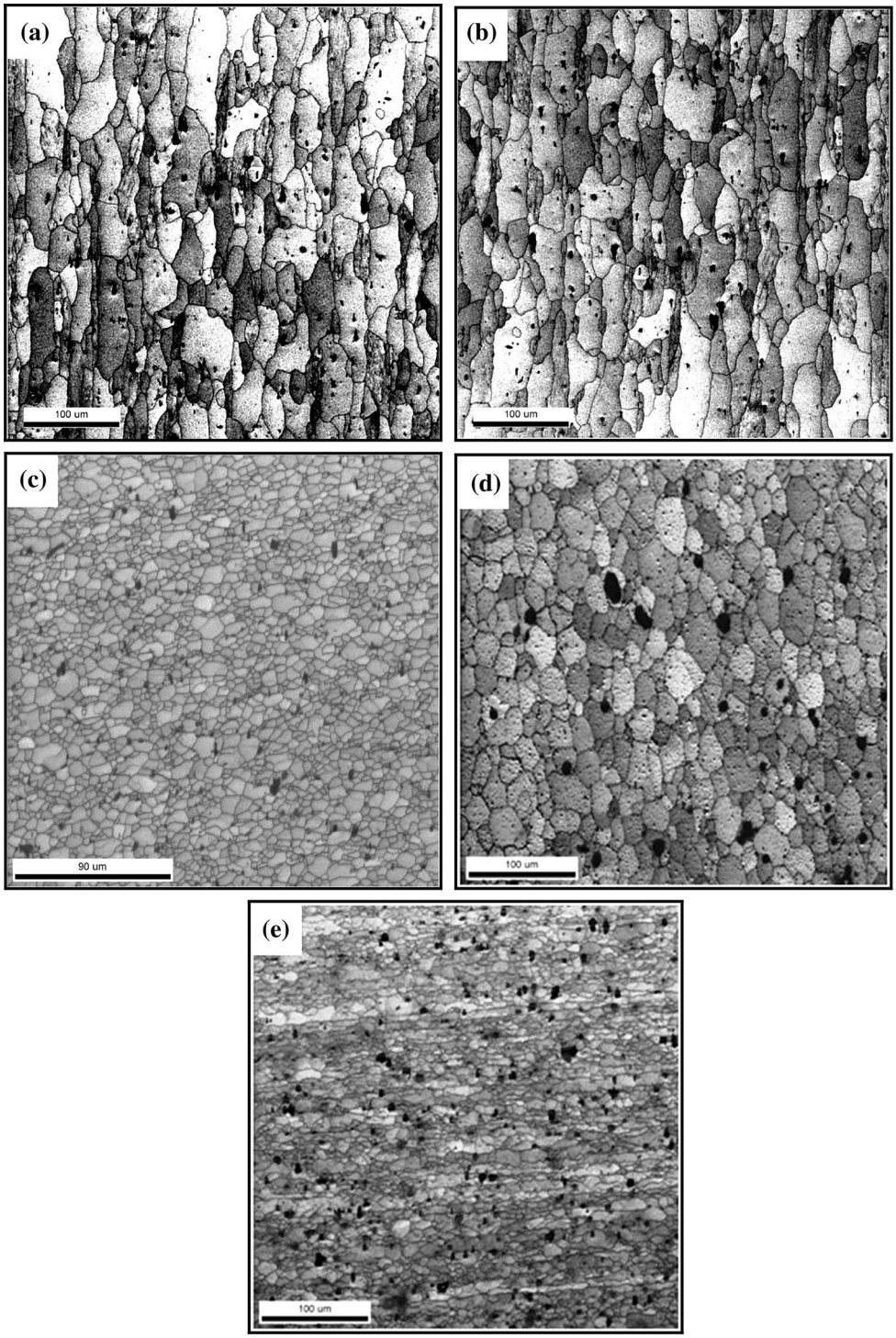

Fig. 6 Processed EBSD map showing grain boundary map of: **a**, **b** tube wall, **c** stir zone, **d** intermediate zone and **e** as received AA6061

alloy. Khorrami and Movahedi [28] called this intermediate zone as static recrystallization zone. The intermediate zone undergoes changes in microstructure during FSBE. The microstructure of the intermediate zone is shown in Figs. 5d and 6d. The grains are equiaxed and bigger compared to stir zone and the parent aluminum alloy. The average grain size is ~26 μm. The intermediate zone is not directly under the rotating tool. Hence, it does not experience considerable deformation leading to dynamic recrystallization. Conversely, the intermediate zone might have experienced static recrystallization. The source can be attributed to the relatively large strain and stored energy present in the initial cylindrical bar obtained from extrusion process. The continuous frictional heating and elevated

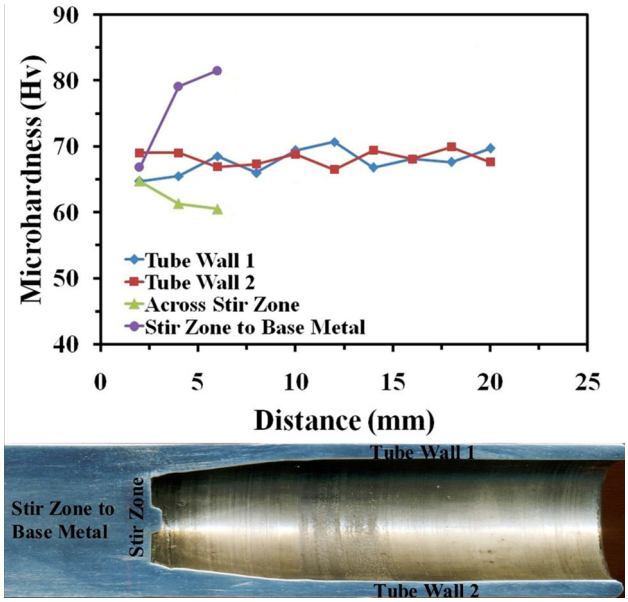

Fig. 7 Microhardness profile across the aluminum tube

temperature prompt the initial strain to supply more nucleation sites for recrystallization [31]. The microstructure of parent aluminum alloy AA6061 is presented in Figs. 5e and 6e. The elongated grains indicate that the aluminum alloy has been processed by conventional extrusion. The average grain size is ~20 μm. The grain size of stir zone is lower compared to base alloy. The FBSE process refines the grain size during stirring and extrusion.

3.3 Microhardness of Aluminum Seamless Tubes

The microhardness across the aluminum seamless tube is shown in Fig. 7. The stir zone records lower microhardness in spite of the fine grained structure. The microhardness of the aluminum seamless tube is slightly higher than the stir zone, but closer to the range of stir zone. The grain size influences the strength of aluminum alloys. Nevertheless, the precipitate distribution is a prevailing strengthening mechanism in heat treatable aluminum alloys [32]. The initial cylindrical bar of aluminum alloy AA6061 is in T6 heat treatment state. The rise in frictional heat and the exposure time is sufficient to overage the precipitates in the aluminum matrix removing the effect of T6 heat treatment. Hence, the microhardness of the stir zone and the tube wall is lower to parent aluminum alloy. Techniques similar to underwater friction stir welding can be used to alleviate the overaging of precipitates and to retain the fine grain structure in the tube wall to enhance the hardness [33]. The microhardness increases from stir zone to parent material due to the presence of precipitates.

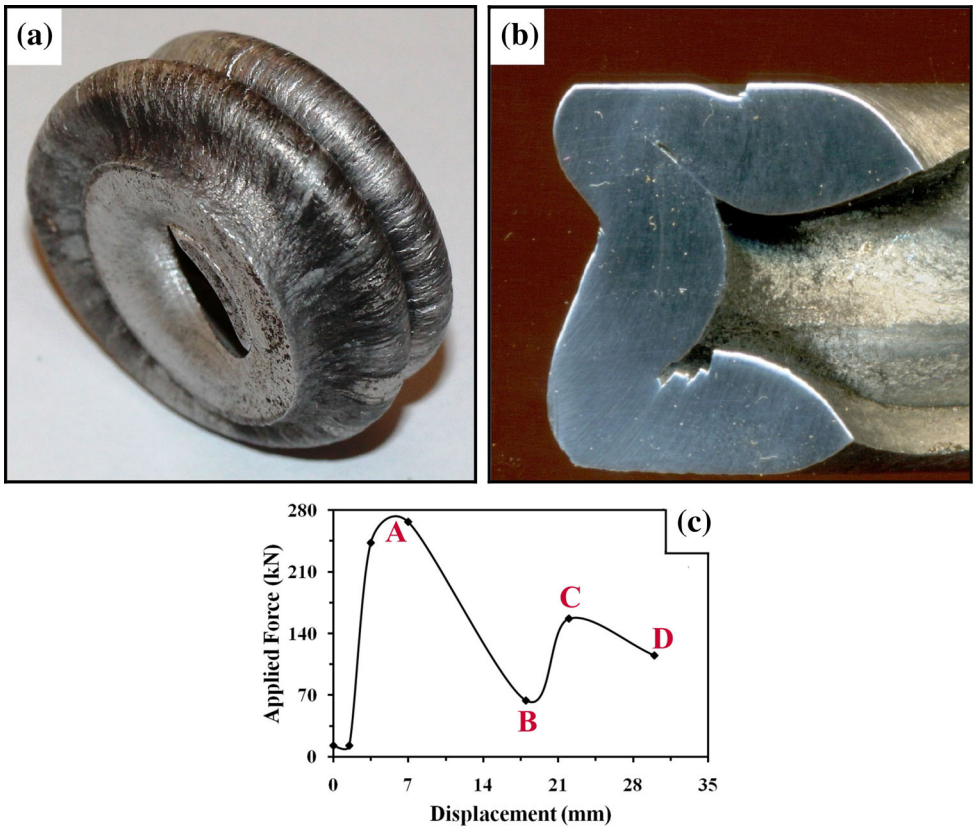

Fig. 8 Photograph of crushed aluminum tube; **a** outer view, **b** cross sectional view and **c** load–displacement curve

3.4 Compressive Strength of Aluminum Seamless Tubes

Aluminum tubes are used as structural members in some applications including automotive frames where they are subjected to crushing loads. Hence, the compression test has been carried out to assess the deformation behavior of the produced aluminum tube. The crushed aluminum seamless tube after the compression test and the load–displacement curve are shown in Fig. 8a. The length to diameter ratio of the compression test tube is 2.1. The mode of failure is concertina or ring mode, which is a preferred mode of failure under crushing of aluminum tubes [34]. A double barrel shape is formed after compression test due to a combination of circumferential stretching and axial bending about circumferential hinges. The crushed aluminum seamless tube shows a high amount of plastic deformation. This aluminum seamless tube produced by FSBE can absorb a considerable amount of energy before failure or on impact as it fails under concertina mode. The polished cross section of the crushed bar (Fig. 8a) shows no visible cracks. The recorded load–displacement curve during compression test is illustrated in Fig. 8c. This curve is characterized with alternate high and low peak loads. The curve reaches the maximum load at point A prior to an axisymmetric deformation. The wall of the tube starts to bend outwards and the force plunges rapidly until the complete formation of the first fold. The force reaches its minimum at point B and begins to rise again. The wall near the deformed zone tends to bend inwards i.e. second fold forms and another force peak at point C appears. Subsequently, the force decreases to point D as the wall bends inwards. The load at the time of double barreling has been found to be 157.6 kN which corresponds to an UCS of 760.1 MPa.

4 Conclusions

AA6061 aluminum seamless tubes were successfully produced by FSBE process. No extrusion defects were seen in the aluminum seamless tubes. The microstructure of the aluminum seamless tube was found to be homogeneous along the tube. The microhardness of the tube was observed to be lower compared to that of the base aluminum alloy due to precipitate overaging. The compressive strength was found to be 760.1 MPa. The aluminum seamless tube failed in concertina mode. The present work established the capability of the FSBE process in producing sound homogeneous aluminum seamless tubes.

Acknowledgments The authors are grateful to Centre for Research in Metallurgy at Karunya University, Welding Research Cell at Coimbatore Institute of Technology and OIM and Texture Lab at Indian Institute of Technology Bombay for providing the facilities to carry out this investigation. The authors are also thankful to Dr. R. Sathis Kumar and Mr. I. Devamanoharan for their assistance offered to execute the above work.

References

1. Mishra R S, and Ma Z Y, *Mater Sci Eng R* **50** (2005) 1.
2. Nandan R, Debroy T, and Bhadeshia H K D H, *Prog Mater Sci* **53** (2008) 980.
3. Threadgill P L, Leonard A J, Shercliff H R, and Withers P J, *Int Mater Rev* **54** (2009) 49.
4. Cao X, and Jahazi M, *Mater Des* **30** (2009) 2033.
5. Shen J J, Liu H J, and Cui F, *Mater Des* **31** (2010) 3937.
6. Song K H, Fujii H, and Nakata K, *Mater Des* **30** (2009) 3972.
7. Bilgin M B, and Meran C, *Mater Des* **33** (2012) 376.
8. Zhou L, Liu H J, and Liu Q W, *Mater Des* **31** (2010) 2631.
9. Sato Y S, Nagahama Y, Mironov S, Kokawa H, Park S H C, and Hirano S, *Scr Mater* **67** (2012) 241.
10. Cavaliere P, Campanile G, Panella F, and Squillace A, *J Mater Process Technol* **180** (2006) 263.
11. Hatamleh O, Lyons J, and Forman R, *Int J Fatigue* **29** (2007) 421.
12. Mishra R S, Mahoney M W, McFadden S X, Mara N A, and Mukherjee A K, *Scr Mater* **42** (1999) 163.
13. Toth L S, and Gu C, *Mater Charact* **92** (2014) 1.
14. Zrnik J, Kovarik T, Novy Z, and Cieslar M, *Mater Sci Eng A* **503** (2009) 126.
15. Toroghinejad M R, Ashrafizadeh F, and Jamaati R, *Mater Sci Eng A* **561** (2013) 145.
16. Zhang W C, Yu Y, Zhang X N, Chen W Z, and Wang E D, *Mater Sci Eng A* **600** (2014) 181.
17. Sarraf S A T, and Langdon T G, *J Alloys Compd* **613** (2014) 357.
18. Zhao Y, Guo H, Fu M W, Ning Y, and Yao Z, *Mater Des* **46** (2013) 889.
19. Pandey S C, Joseph M A, Pradeep M S, Raghavendra K, Ranganath V R, Venkateswarlu K, and Langdon T G, *Mater Sci Eng A* **534** (2012) 282.
20. Mohebbi M S, and Akbarzadeh A, *Mater Sci Eng A* **528** (2010) 180.
21. Farshidi M H, Kazeminezhad M, and Miyamoto H, *Mater Sci Eng A* **615** (2014) 139.
22. Arzaghi M, Fundenbergera J J, Toth L S, Arruffat R, Faure L, Beausir B, and Sauvage X, *Acta Mater* **60** (2012) 4393.
23. Mesbaha M, Farajib G, and Bushroa A R, *Mater Sci Eng A* **590** (2014) 289.
24. Ma Z Y, *Metall Mater Trans A* **39** (2008) 642.
25. Farha F A, *Scr Mater* **66** (2012) 615.
26. Milner J L, and Farha A F, in *Magnesium Technology*, (eds) Alderman M, Manuel M V, Hort N, and Neelameggham N R, Wiley, Hoboken (2014), p 497.
27. Dinaharan I, Sathiskumar R, Vijay S J, and Murugan N, *Proced Mater Sci* **5** (2014) 1502.
28. Khorrami M S, and Movahedi M, *Mater Des* **65** (2015) 74.
29. Chang S C, Wang C C, Huang C A, Chang Y, and Chen T L, *J Mater Process Technol* **108** (2001) 294.
30. Liu G, Murr L E, Niou C S, McClure J C, and Vega F R, *Scr Mater* **37** (1997) 355.
31. Khorrami M S, Kazeminezhad M, and Kokabi AH, *Mater Des* **40** (2012) 364.
32. Reddy G M, Mastanaiah P, Satyaprasad K, and Mohandas T, *Trans Indian Inst Met* **62** (2009) 49.
33. Zhang H J, Liu H J, and Yu L, *Sci Technol Weld Join* **16** (2011) 459.
34. Reid S R, *Int J Mech Sci* **35** (1993) 1035.